Viable Adaptive Neural Network Controller for STATCOM in Stand-Alone Wind Power System

Ahmed A. A. Hafez, R. M. Al-Bouthig and J. I. AL-Sadey
Department of Electrical Engineering
University of Assiut
Assiut, P.O. 715164, Egypt
elhafez@aun.edu.eg

***Abstract* – Reliable and viable controller based on neural network for STATCOM in off-line wind power system is advised. A simple adaptive neural extraction circuit is used for generating the reference currents from the load currents. Levenberg-Marquardt back propagation was used for training the advised neural control. The advised control enjoys the advantages of simplicity and reliability. The proposed controller was corroborated through comprehensive simulation results in Matlab environment under rigorous operating regimes. The results verified the flexibility and feasibility of the proposed control strategy.**

Index-terms- ***Adaptive Neural Network, STATCOM, Self-Excited Induction Generator, Back Propagation.***

I. INTRODUCTION

Recently, wind-based electricity is penetrating progressively the power system. This is attributed to the merits of reliability, sustainability and environmental compatibility of such systems [1].

The Induction Generator (IG) is the most preferable generator option in wind systems, due to its salient features of robustness, simplicity and absence of DC-excitation system [2].

In stand-alone wind power system, the IG is commonly themed as Self-Excited IG (SEIG). Its reactive power requirements are supplied from an external source, mostly capacitor bank installed at the machine terminals [3]. However, this scheme of excitation has the drawback of the difficulty to control voltage/frequency under variable load conditions. For example, a change in the load power may result in large voltage transients and even instability [3]. To avoid this drawback, the capacitor bank is replaced or augmented by power electronics based reactive power compensators [2].

Static Synchronous Compensator (STATCOM) was emerged recently as an alternative for conventional static reactive power compensators as Static VAR Compensator (SVC) and Thyritsor-Controlled Reactors (TCR) [4-6]. The STATCOM has the ability of continuous control for the flow of reactive power without dependency on the AC system voltage, which could stabilize a power system, increase the transferred active power and regulate the system voltages. As, the STATCOM is usually parallel connected, it enjoys reduced volumetric dimension and rating. STATCOM could also be deployed for harmonic cancellation, load balancing and improving power quality [4-6].

Various control methods are reported in the literature for controlling STATCOM, some of which rely on conventional Proportional and Integral (PI) control [7-10]. This was attributed to the merits of simple concept, convenient adjustment and easy realization of PI control. However, these methods [7-10] suffer from a deteriorate performance, particularly during/following large disturbances [7-10].

To overcome the limitations that encompass the conventional methods, novel techniques are emerged. Adaptive Neural Network (ANN) controls have the ability of adapting themselves for the problem to be solved, despite the lack of precise mathematical models [11-19]. These methods are imitating brain and neural system of the humans. Thus various terminologies for NN control were derived from the biological neural networks, for example, neurons.

Generally ANN is composed of a finite number of neurons, which are interlinked to each other. Synaptic weights are used to measure the strength of the connections. NN has the merit of learning from its environment to improve its performance. Elaborate processes of adjustments for the entangled weights maintain the continuity of the performance improvement. As the learning process goes through, the NN becomes more knowledgeable about its environment. Different techniques are adopted for learning of NN, as error back propagation and Levenberg-Marquardt Back Propagation (LMBP) [11-19].

This article advises an ANN control for STATCOM in stand-alone wind power system. The NN has two main parts: extraction circuit and the main controller. The extraction circuit extracts the reactive and harmonic components from the sensed load currents. Main controller synthesizes reference currents and then compares them with the actual currents to generate the switches driving signals. Levenberg-Marquardt back propagation was used for training the advised neural control. The simulation model of the system under concern with the advised control is built in MATLAB dynamic simulation platform. The proposed ANN control has the advantages of reliability and robustness. The viability and simplicity of such control were corroborated against severe operating scenarios. The system was loaded by nonlinear, resistive and inductive linear loads.

II. STAND-ALONE WIND POWER SYSTEM

In the system under concern, three-phase SEIG is driven from a wind turbine, Fig. 1. A capacitor bank at the terminals of the generator is used for fulfilling the generator reactive power at unity power factor rated load condition. To provide the load requirements of reactive power, three-phase STATCOM is connected near the load. A short transmission line of 60km connects the wind farm to the load. Simple low pass filters are inserted between the STATCOM output and the Point of Common Coupling (PCC). This is to filter out the high frequency switching ripples. Normally, the STATCOM is coupled to the system through a transformer, which may eliminate the need for the inductor filter. The STATCOM is implemented by three single-phase star-connected H-bridge inverters. As each phase is individually controlled; this creates extra degree of freedom and extends the applicability of STATCOM for different operating scenarios such as load balancing. Moreover, the inverter topology in Fig. 1 improves the modularity. However, it is worth to mention that the inverter topology in Fig.1 may suffer from increased component count and hence cost. The parameters of the system under concern are given in Table1.

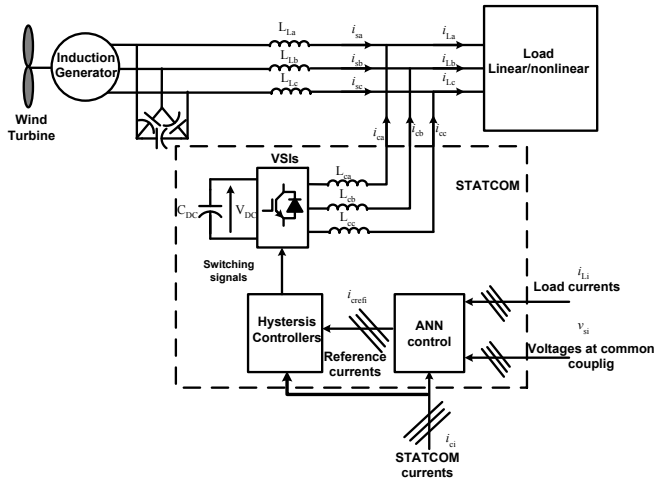

Fig.1 Schematic for stand-alone wind power system equipped with STATCOM

Fig. 1 shows that load currents i_{Li} and voltages at common coupling point are measured, conditioned and manipulated by the advised ANN control. The compensated components of the load current are extracted; then reference currents are generated. Then, reference currents and STATCOM currents are compared through hysteresis band, to generate switching signals for the switches, Fig. 1.

TABLE 1
SYSTEM PARAMTERS

Parameters of IG	4pole, 75kW, Y, 400V,50Hz,
Stator resistance and reactance respectively	0.0355 Ω , 0.1052Ω
Rotor resistance and reactance respectively	0.0209 Ω,0.1052 Ω
Magnetizing reactance	4.8Ω
Inductance of the transmission line per unit length	0.64mH/km
Inductance of the coupling magnetic	8mH

a. Modeling of wind turbine

The mechanical output power of a wind turbine, P_{mech}, is a function in wind speed, v_{wind}, air density ρ, area swept by the turbine A, and turbine performance coefficient C_p , [20,21],as given by,

$$P_{mech} = C_P(\lambda,\beta)\frac{\rho A}{2}\upsilon_{wind} \qquad (1)$$

The power coefficient C_p, (1), depends on tip-speed ratio of the rotor, λ , and pitch angle, β , as shown by,

$$C_p = 0.22(116x_{\lambda,\beta} - 0.4\beta - 5)e^{-12.5x_{\lambda,\beta}} + 0.0068\lambda \qquad (2)$$

where $x_{\lambda\beta}$ is also a function in λ and β as revealed by,

$$\frac{1}{x_{\lambda,\beta}} = \frac{1}{\lambda + 0.08\beta} - \frac{0.035}{1+\beta^3} \qquad (3)$$

The dependency of the turbine performance coefficient on tip-speed ratio of the rotor and pitch angle can be exposed clearly in Fig. 2.

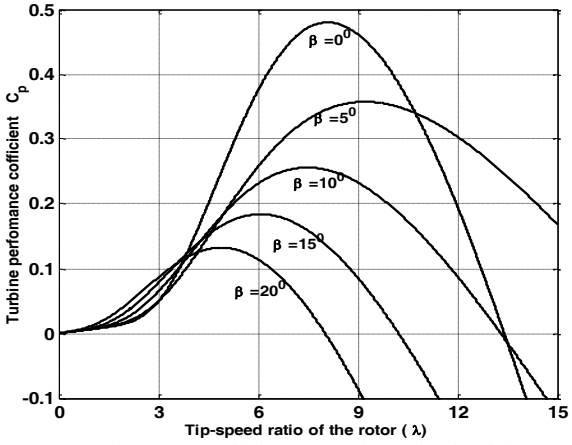

Fig. 2 Power performance coefficient versus tip-sped ratio of the rotor for different pitch angle

The turbine coefficient and hence its mechanical power could be controlled by adjusting pitch angle. Moreover, maximum power is occurred at zero pitch angle, Fig. 2.

The characteristics of the turbine that drives SEIG under concern are shown in Fig. 3, at different wind speeds for zero pitch angle. The wind speed of 10m/sec is taken as the base speed.

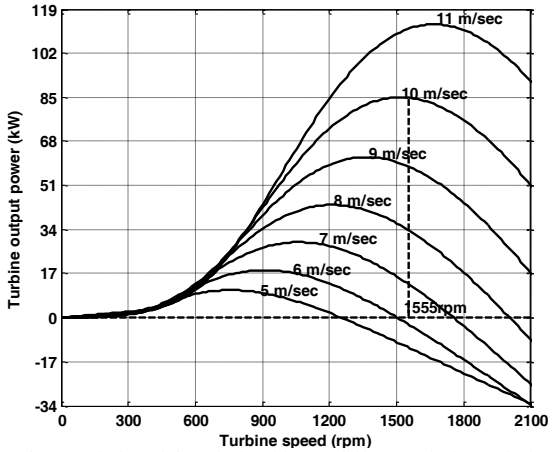

Fig. 3 characteristics of the wind turbine at different wind speeds for zero pitch angle

In this research, the turbine is modeled according to equations (1)-(3) and Figures 2 and 3. Variable pitch angle control is employed for regulating the turbine output mechanical power. For the turbine to deliver maximum power, the pitch angle is set to zero. However, for system operation at reduced power levels, the pitch angle is adjusted.

III. ADVISED ADAPTIVE NEURAL NETOWRK CONTROL

Single-line diagram for system under concern is shown in Fig. 4.

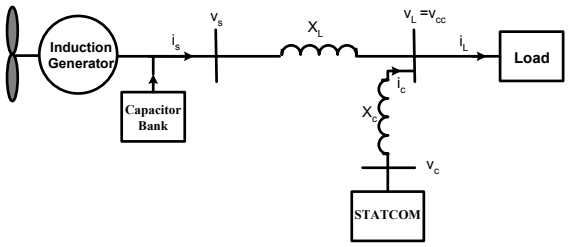

Fig.4 Schematic for stand-alone wind power system equipped with STATCOM

where V_s , V_L and V_c are generator/supply, load and STATCOM terminal voltages respectively. i_s, i_L and i_c are generator, load and STATCOM currents respectively. Here in this research, the voltage at common coupling point V_{cc} is equal to load voltage V_L .X_L and X_c are reactance of positive sequence of the transmission line and equivalent reactance for low pass filter and coupling transformer respectively.

STATCOM complex power, S_c, is given by [4],

$$S_c=\frac{3V_cV_{cc}}{X_c}\sin(\delta)-j\left(\frac{3V_cV_{cc}}{X_c}\cos(\delta)-\frac{3V_{cc}^2}{X_c}\right) \quad (4)$$

where δ is the angle between STATCOM voltage and voltage at common coupling point. Ideally, δ=0, thus the STATCOM reactive power is given by,

$$Q_c=\frac{3V_{cc}}{X_c}(V_c-V_{cc}) \quad (5)$$

The direction/sign of reactive power flow depends on magnitude of STATCOM voltage, V_c, relative to the voltage of common coupling point, V_{cc}. Thus, STATCOM voltage, V_c, has to be more than voltage at common coupling, V_{cc}, to produce reactive power.

For the system under concern, phasor diagram for case of an inductive linear load is shown in Fig. 5. In this scenario, the harmonic component of load current is equal to zero.

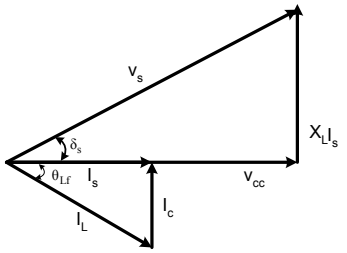

Fig.5 phasor diagram for fundamental component of the currents and voltages of system under concern in case of inductive linear load

δ_s and θ_{Lf} are angle of generator voltage relative to common coupling point voltage and angle of fundamental component of load current respectively.

The phasor diagram, Fig. 5, indicates that even for resistive load, the generator current lags its voltage. The generator terminal voltage has to be slightly greater than voltage at common coupling; this is to fulfill the reactive power requirements of the transmission line. Thus, the fixed excitation arrangement should be sized according to the reactive power demands of the generator and the transmission line.

a. Principles of advised adaptive neural network control for STATCOM

Per-phase equivalent circuit of the generator, STATCOM and a generic load is illustrated in Fig. 6. The generator is modeled as sinusoidal source with voltage v_s and current i_s. STATCOM is depicted here as variable DC source uV_{DC}. V_{DC} is the voltage of the energy storage arrangement on the DC-link of the STATCOM, while u is defined according to the modulation strategy. u typically is either 1 or -1, as hysteresis band controller is adopted for generating switching signals. L_f represents low pass filter, which interfaces STATCOM to PCC.

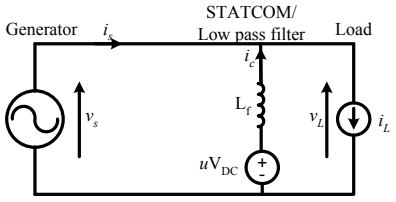

Fig.6 Per-phase equivalent circuit of STATCOM, load and generator

A generic load is considered in Fig. 6, which is modeled as current source i_L . i_L is given by,

$$i_L(t)=I_{Lf}\sin(\omega t-\theta_{Lf})+\sum_{h=3,5,}^{\infty}I_{Lh}\sin(h\omega t-\theta_{Lh})=$$
$$I_{Lf}\sin(\omega t)\cos(\theta_{Lf})-I_{Lf}\sin\left(\omega t+\frac{\pi}{2}\right)\sin(\theta_{Lf})+$$
$$\sum_{h=3,5,}^{\infty}I_{Lh}\sin(h\omega t-\theta_{Lh})=i_{Lfp}(t)+i_{Lfq}(t)+i_{Lh}(t) \quad (6)$$

where I_{LF} is amplitude of fundamental load current component. I_{Lh} and θ_{Lh} are amplitude and phase of h harmonic components. i_{Lfp}, i_{Lfq} and i_{Lh} are instantaneous active, reactive and harmonic components of load current respectively.

The load current i_L, (6), has fundamental and harmonic components. The harmonic component disappears for linear loads. The fundamental component could be expressed further by two components. One represents, i_{Lfp}, the active power and it is phase with the supply voltage, while the other, , i_{Lfq}, stands for reactive power and it is 90^o out of phase with the supply voltage.

STATCOM principally controls voltage at PCC through instantaneous injection of reactive power. However, it could be also deployed for filtering the harmonics in the load. Thus, the supply pumps only active current

component to the load; and then the STATCOM current i_c is expressed by,

$$i_c(t)=i_L(t)-i_{Lfp}(t)=i_L(t)-I_{Lf}\sin(\omega t)\cos(\theta_{Lf}) \quad (7)$$

In the proposed control, STATCOM under inductive linear load compensates inductive current components; thus, STATCOM current leads load voltage by $\pi/2$, Fig. 4.

Assuming that supply voltage, $v_s(t)$, is sinusoidal with amplitude V_m . Supply voltage is taken as a reference. Defining W as,

$$W=\frac{I_{Lf}\cos(\theta_{Lf})}{V_m} \quad (8)$$

Substituting (8) into (7) and rearranging, the STATCOM current i_c is given by,

$$i_c(t)=i_L(t)-Wv_s(t) \quad (9)$$

W is calculated from adaptive neural network, as shown in Fig. 7.

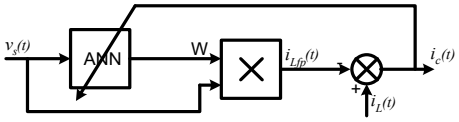

Fig. 7 Synthesize of STATCOM current

where ANN stands for adaptive neural network. The ANN consists of a neuron that is an adaptive linear element. The weight of the neuron is equivalent to W, and the bias is equivalent to zero. The input for ANN is supply voltage $v_s(t)$, and the output is STATCOM current i_c . According to the Widrow-Hoff learning rule, the updated weight is given by,

$$W(k)=W(k+1)+\gamma i_c v_s(k-1) \quad (10)$$

where $\gamma i_c v_s(k-1)$ represents the change of the weight at kth sampling; γ is the learning rate that has a value between 0 and 1. i_c is the reference compensating current of the STATCOM,

$$i_c(k)=i_L(k)-W(k)v_s(k) \quad (11)$$

Equations (7) to (11) are modeled in Fig. 8.

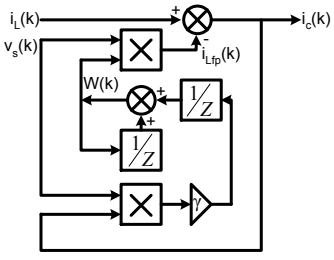

Fig. 8 Synthesis of reference current for STATCOM

The generic principle of the advised control is depicted in equations (7) to (11). The reference current of the STATCOM is synthesized from load current and the voltage at the common coupling through ANN.

The schematic diagram for stand-alone wind power system with ANN for controlling the STATCOM is shown in Fig. 9.

The load current and the voltage at the common coupling are sensed and fed to extraction circuit based on ANN. The output of the extraction circuit is reactive and harmonic components in load current, which are compensated by the STATCOM, Fig. 9.

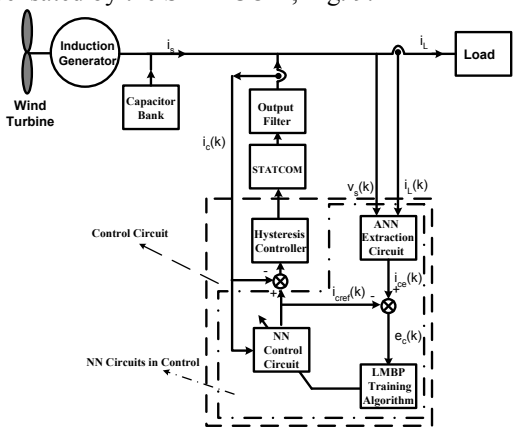

Fig. 9 Off-line wind power system with the proposed control for STATCOM

The current from the extraction circuit is compared with the current from NN control circuit to generate error signal. This signal is manipulated through Levenberg-Marquardt Back Propagation (LMBP) training algorithm to drive NN control circuit. The output of NN control circuit is compared with the STATCOM output current through hysteresis controller to generate switching signal for switches in the STATCOM.

b. Neural network controller design

The neural network controller is feed-forward network. It consists of the input, hidden and output layers, Fig. 9. The input layer stores all the input data and the hidden layer performs all the computations. Each circle in the hidden layer represents a neuron, Fig. 10, where *w* is the weight attached to each neuron, *b* and *f* are the bias and the activation function respectively. The results of the computations are stored in the output layer, which has also an activation function *f* of sigmoid .The function of this neural network controller is to ensure that the Root Mean Square (RMS) value of the STATCOM current $i_c(k)$ converges to the root mean RMS value of the compensated current, so that the harmonics and the reactive component of the fundamental can be cancelled in the load current. This neural network controller is trained using LMBP.

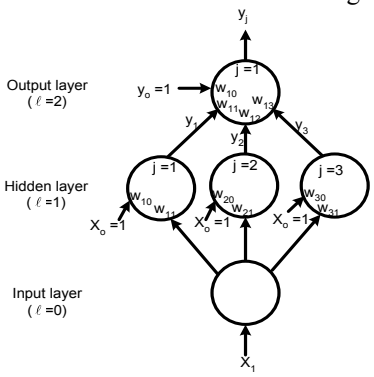

Fig.10: Three layer feed-forward neural network

LMBP is different from the error back propagation, as it uses resulting derivatives for the weights updating. The LMBP algorithm is well-suited for neural network

training, where the performance function is the mean square error. As in the standard back propagation algorithm, this LMBP algorithm also has forward pass and backward pass. During the forward pass, it calculates the model output error for the given data set by fixing the weights. The weights are updated in the backward pass in order to make the model response equal to the desired response. The back propagation process continues until all the weights have been adjusted. Then, using a new set of inputs, information is fed forward through the network (using the new weights) and the errors at the output layer computed [22, 23]. The process continues until:

1. The performance function reaches an acceptable low values.
2. A maximum iteration count has been exceeded.
3. A training time period has been exceeded.

If 2 or 3 occurred, while only a local minimal is reached. Then, the back propagation may be restarted, if and again unsuccessful, a new training set may be required.

In the neural network shown Fig. 10 , the current input x_1 represents the RMS value of the STATCOM output current. The desired output y_i is the RMS value of the desired signal of the extraction circuit. The difference between the desired signal and the output signal of neural network controller is used to update the weights and biases of the controller.

Assuming the value of the learning rate is γ =0.5. The equations that govern the NN control circuit are summarized as follows: For the hidden layers (ℓ =1), the law of single neuron summation, [23], is given by,

$$s_j=\sum_{i=1}^{N} w_{ji}x_i+b_j \tag{12}$$

where s_j is the weight sum; bj and wji are the bias and the weight respectively. For the three neurons, , Fig. 8, (j=1, 2,3), (12) could be expressed in matrix form as,

$$\begin{bmatrix} s_1 \\ s_2 \\ s_3 \end{bmatrix}=\begin{bmatrix} w_{11} \\ w_{21} \\ w_{31} \end{bmatrix}x_i+\begin{bmatrix} w_{10} \\ w_{20} \\ w_{30} \end{bmatrix} \tag{13}$$

The values of weights and biases in hidden layers are assumed as initial values. Sigmoid activation functions for the output layer (j=1),

$$y_j=y_1=\frac{1}{1+e^{-s_j}} \tag{14}$$

where y_j is the neuron output. For, the output layer (ℓ =2), the single neuron s_1 is given by,

$$s_1 = w_{10} + w_{11}y_1 + w_{12}y_2 + w_{13}y_3 \tag{15}$$

For LMBP back propagation training algorithm, the governing equations are given in the following section. For output layer, (ℓ =2), the error e_c is calculated, which is the difference between the desired signal and the output of neural network.

$$e_c=d_j-y_j \tag{16}$$

$$\delta_j=y_j\left(1-y_j\right)e_c \tag{17}$$

where δ_j is function in error in the output layer; since (j=1), the δ_1 is given by,

$$\delta_1=y_1\left(1-y_1\right)\left(d_1-y_1\right) \tag{18}$$

Using delta rule to update the weights and the biases of the output layer,

$$\Delta w_{ji}(kt)=\gamma\delta_j x_i \tag{19}$$

where $\Delta w_{ji}(kt)$ is the weighted increment, which is called delta rule, [23]. New weights and biases for the output layer are given by,

$$w_{ji}(kt)=w_{ji}(1-k)t+\Delta w_{ji}(kt) \tag{20}$$

For the hidden layers, (ℓ =1), the values of $\left[\delta_j\right]_\ell$ are given by,

$$\left[\delta_j\right]_\ell = \left[y_j(1-y_j)\right]_\ell \left[\sum_{}^{N} w_{ji}\delta_j\right]_\ell \tag{21}$$

The δ_i values for layer ℓ for only a single neuron in layer (ℓ +1)

$$(j=1) \quad \left[\delta_1\right]_\ell = \left[y_1(1-y_1)\right]_\ell \left[w_{ji}\delta_j\right]_\ell \tag{22}$$

$$(j=2) \quad \left[\delta_2\right]_\ell = \left[y_2(1-y_2)\right]_\ell \left[w_{ji}\delta_j\right]_\ell \tag{23}$$

$$(j=3) \quad \left[\delta_3\right]_\ell = \left[y_3(1-y_3)\right]_\ell \left[w_{ji}\delta_j\right]_\ell \tag{24}$$

Hence, using the delta rule, the weight increments for the hidden layer are:

$$\Delta w_{10}=\gamma\delta_1 x_0 \tag{25}$$

$$\Delta w_{20}=\gamma\delta_2 x_0 \tag{26}$$

$$\Delta w_{30}=\gamma\delta_3 x_0 \tag{27}$$

$$\Delta w_{11}=\gamma\delta_1 x_1 \tag{28}$$

$$\Delta w_{21}=\gamma\delta_2 x_1 \tag{29}$$

$$\Delta w_{31}=\gamma\delta_3 x_1 \tag{30}$$

The new weights and biases for the hidden layer are updated according to the equation (20). The process will continue until the performance function has low value.

III. CONTROL VALIDATION

To validate the advised control a simulation model of the system under concern, Fig. 1, with the ANN control is built in MATLAB/Simulink. The wind turbine is modeled as mentioned before according to Figs. 2 and 3 and equations (1)-(3). It is modeled by a set of lockup tables that accepts load power, wind and generator speed while produces the driving torque. The following operating scenario is applied to the system in Fig. 1. The system initially was loaded by 25kW unity power factor load. At 1sec a nonlinear load was suddenly connected, while the machine is load by 25kW resistive load. Then, the nonlinear is disconnected at 1.4sec. The nonlinear load is modeled by a three-phase diode rectifier loaded with R-L load, where the resistance R is 2.5Ω, and the inductance L is 20mH. This load absorbs nearly 25kW active power. The load voltage and current of three-phase diode rectifier are approximately DC. At 1.6sec , 55kW, 0.75pf lag load was also suddenly applied. The load active and reactive powers are plotted. Also, generator, load and STATCOM currents are illustrated. Generator torque and speed are drawn. Moreover, the error extracted compensated signals are illustrated.

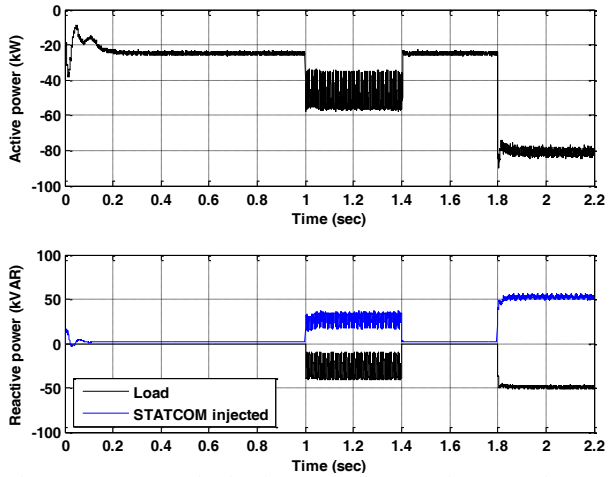

Fig. 11 Instantaneous load active power (top), reactive power (bottom): load (blue) and STATCOM injected (black); for nonlinear load injection at 1sec and disconnection at 1.4sec; 55kW inductive linear load injection at 0.75pf lag at 1.6sec.

Fig 11 shows the instantaneous power of the load during the simulated time span. The ripples either in active or reactive powers in the period 1sec to 1.4sec are attributed to the operation of the nonlinear load. Reactive power of the load, bottom graph, is nearly compensated by STATCOM.

During the periods of resistive load, the STATCOM is floating neither inject nor absorb reactive, Fig. 10. This validates the analysis particularly equations (7)-(11).

During the interval of 1.8sec-2.2sec, the wind turbine operates at maximum operating point. As mentioned before, the pitch angle is kept at zero to achieve such conditions.

Load, STATCOM and generated currents are shown in Figs.12 and 13. Fig. 13 is incorporated to reveal obviously the ability of the proposed control in compensating harmonics of the load currents.

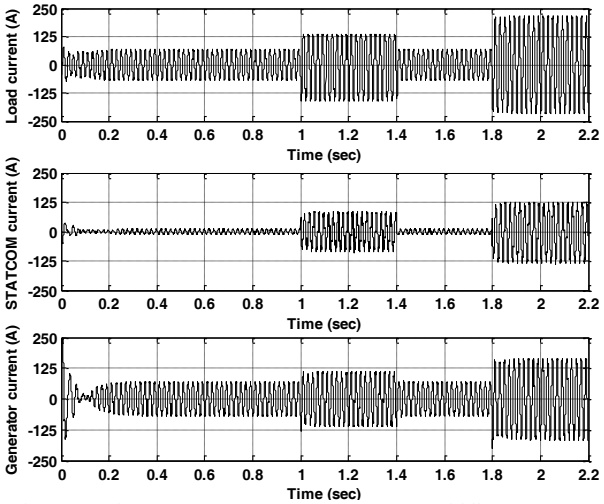

Fig. 12 Load current (Top), STATCOM current (middle) ,Generator current (bottom), for nonlinear load injection at 1sec and disconnection at 1.4sec; 55kW inductive linear load injection at 0.75pf lag at 1.6sec.

Fig. 12 demonstrates the adequate response of the STATCOM with the advised ANN control for rigorous operating scenarios. At 1sec, a nonlinear load of around 25kW was suddenly injected to the system. STATCOM as shown in Figs. 11 and 12 reacts almost instantaneously to fulfill load reactive power requirements and to filter out the harmonics in the load current. Moreover, at 1.8sec, 55kW at 0.75pf lag load is abruptly applied to the system. STATCOM, again reacts by pumping around 50kVAR to the load, Fig. 11. During resistive load periods, 0-1sec and 1.4-1.8sec, STATCOM generates nearly zero reactive power, Figs. 10 and 11, which concurs with the criterion of compensation, (7)-(11).

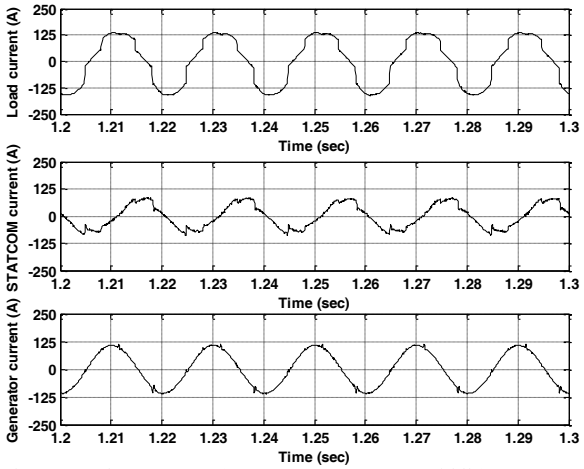

Fig. 13 Load current (Top), STATCOM current (middle) ,Generator current (bottom), for nonlinear load for 1.2-1.3sec time span.

Fig. 13 shows load, STATCOM and generator over 100msec of nonlinear time span. The load current is distorted, top graph Fig. 13, while the generator current is nearly sinusoidal. Thus, STATCOM successfully attenuates harmonics of the load current. The spikes in the STATCOM and generator currents are attributed to commutation in the three-phase diode rectifier, nonlinear load.

Fig. 13 corroborates the feasibility of the proposed control, particularly its ability in suppressing the harmonics.

Generator, fundamental component of STATCOM and load voltages are shown in Fig. 14.

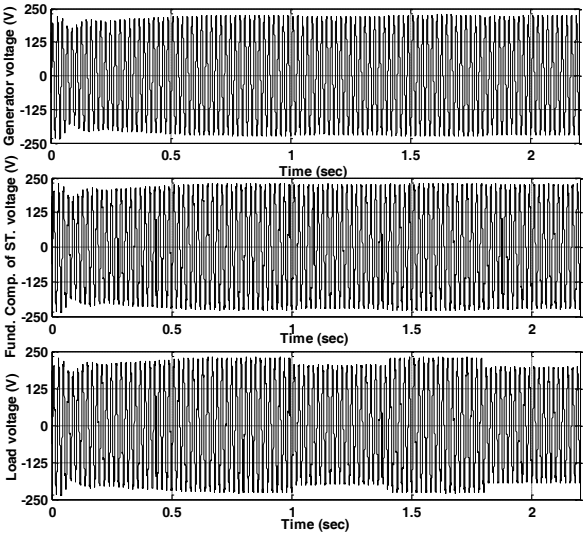

Fig. 14 Generator voltage (Top), STATCOM voltage (middle) ,load voltage (bottom), for nonlinear load injection at 1sec and disconnection at 1.4sec; 55kW inductive linear load injection at 0.75pf lag at 1.6sec.

Fig. 14 shows that load voltage experience a drop during nonlinear and linear inductive loads operation. STATCOM voltage under such conditions is greater than load voltage, Fig. 14, which ensures reactive power flow from STATCOM to the load. This correlates (4).

Generator and STATCOM voltages nearly are equal; this implies that STATCOM is not contributing in fulfilling reactive power requirements of the generator. They are realized by capacitor bank at the terminal of the generator.

Voltage and current of the load in the DC side of nonlinear diode rectifier load are illustrated in Fig. 15.

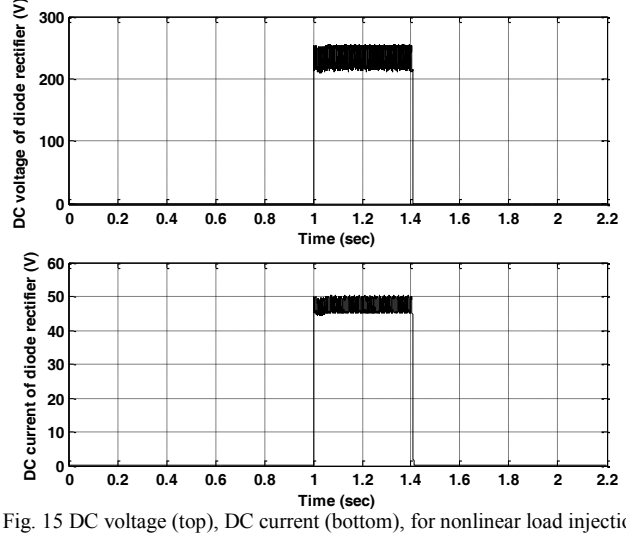

Fig. 15 DC voltage (top), DC current (bottom), for nonlinear load injection at 1sec and disconnection at 1.4sec; 55kW inductive linear load injection at 0.75pf lag at 1.6sec.

Fig. 15 indicates that load inductance is sufficiently large, thus the load current/voltage are approximately constant.

Turbine torque , generator torque and speed are illustrated in Fig. 16.

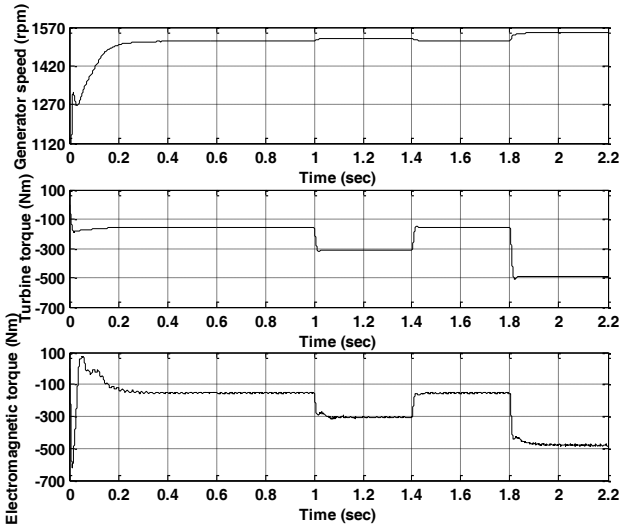

Fig. 16 Generator speed (top), Turbine torque Nm (middle), electro-magnetic torque Nm (bottom); for nonlinear load injection at 1sec and disconnection at 1.4sec; 55kW inductive linear load injection at 0.75pf lag at 1.6sec.

The operating slips are approximately 0.008, 0.018 and 0.033 for resistive, nonlinear and inductive loads respectively. The machine under concern is a low slip machine, as slip at maximum torque is around 0.098. This may attributed to low value of the rotor resistance.

As mentioned, for system operation at maximum captured wind power, the pitch angle is settled to zero. However, for the operation at reduced load levels, pitch angle controller was adapted in order to achieve power balance, as the system is isolated and no energy storage elements were deployed.

The error signal, E_c, and the RMS values for the STATCOM current and the compensated components extracted from the load current are given in Fig. 16.

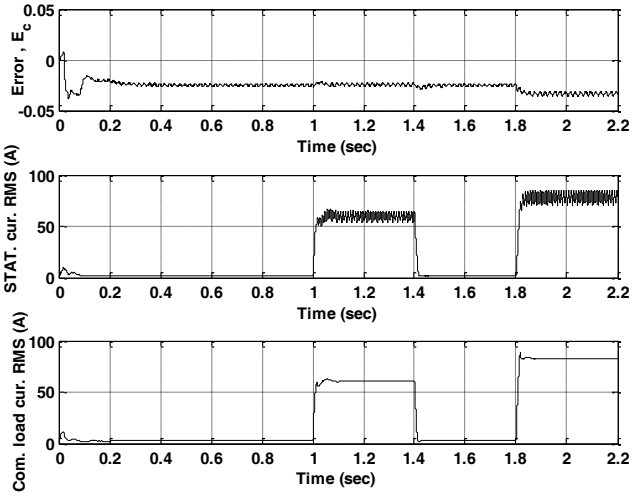

Fig. 17 Error signal E_c (top), RMS value of STATCOM current (middle), RMS value of the compensated load current components (bottom); for nonlinear load injection at 1sec and disconnection at 1.4sec; 55kW inductive linear load injection at 0.75pf lag at 1.6sec.

The error signal E_c, (16), is nearly zero, Fig. 17, even during system operation with full load power. The proposed ANN control forces the RMS value of the STATCOM current to track reference value, Fig. 17. This reveals the viability, reliability and robustness of the advised control.

VI. CONCLUSION

A reliable ANN control for STATCOM in off-line wind power system was advised. A Detailed analysis for the design of the NN control is given. In the proposed control, the reference current is synthesized from load current and voltage at common coupling point. Then, it is compared with the STATCOM current to generate driving signals of the switches.. LMBP was used for training the advised neural control. LMBP is more robust than error back propagation. Severe operating regimes are used for validating the proposed ANN control. The simulation results corroborated the flexibility and viability of the advised control strategy.

A number of conclusions could be extracted:

1. Fixed excitation capacitance at the terminals of the SEIG could not fulfill the generator/load reactive power requirements under variable load conditions.
2. For STATCOM to produce capacitive reactive power, its voltage has to be greater than that of coupling point.

3. The advised ANN control instantaneously compensates load reactive power, while filters out the harmonics of load current.
4. A simple and reliable ANN extraction circuit was employed for generating reference current from load currents.
5. STATCOM with the proposed control is not contributing in fulfilling generator or transmission line reactive power demand.
6. A separate arrangement is employed for regulating the DC-side voltage of the STATCOM, which may added to the cost of the system.
7. Instead of tracking RMS value, the instantaneous values of the compensated currents should be tracked. This possibly enhances the performance of the proposed NN control.

REFERENCES

[1] Chen, Z. and F., Blaabjerg "Wind farm—A power source in future power systems". *Renewable and Sustainable Energy Reviews*, Vol. 13, no 6, pp. 1288-1300, 2008.

[2] Bansal, R. C.; Bhatti, T. S. and Kothari, D. P. "A bibliographical survey on induction generators for application of nonconventional energy systems", *IEEE Transaction on Energy Conversion*., vol. 18, no. 3, pp. 433–439, Sep. 2003.

[3] Idjdarene, K. ; Rekioua, D. ; Rekioua, T. and Tounzi, A. "Performance of an Isolated Induction Generator Under Unbalanced Loads "*IEEE Transactions on Energy Conversion,* vol. 25 ,no. 2 , pp. 303-311, 2010.

[4] Singh, B. ; Saha, R.; Chandra, A. and Al-Haddad, K." Static synchronous compensators (STATCOM): a review" *IET Power Electron*, vol. 2, no. 4, pp. 297–324, 2009.

[5] Dhal, P.K. and Rajan, C.C.A."Transient stability improvement using neuro-fuzzy controller design for STATCOM" International Conference on Advances in Engineering, Science and Management (ICAESM), 2012 , pp. 510-515, 2012.

[6] Al-Bouthigy, R. T.; hafez, A. A. and Al-Sadey, I." Robust STATCOM Control Design Using P-Q theory for Wind Driven Induction Generator" Accepted and to be appear in *Journal of Electrical Engineering*, vol. 14, 2014.

[7] JOSH K., BEHALF A., JAIN A.K. and MOHAN N.: 'A comparative study of control strategies for fast voltage regulation with STATCOMs'. 30th IEEE Annual Conf. Industrial Electronics Society, IECON, 2004, vol. 1, pp. 187–192.

[8] Kuiava, R. ; Ramos, R.A. and Bretas, N.G."Control design of a STATCOM with Energy Storage System for stability and power quality improvements "IEEE International Conference on Industrial Technology, 2009, ICIT 2009, pp. 1-6, 2009.

[9] JAIN A., JOSHI K., BEHAL A. and MOHAN N.: 'Voltage regulation with STATCOMs: modeling, control and results', *IEEE Transaction of Power Delivery*, 2006, vol. 21, no. 2, pp. 726–735, 2006.

[10] VORAPHONPIPUT N. and CHATRATANA S.: 'STATCOM analysis and controller design for power system voltage regulation'. IEEE/PES Transmission and Distribution Conference Exhibition: Asia and Pacific, 2005, pp. 1–6.

[11] Shaojian Song ; Yi He ; Xiaofeng Lin and Bilian Liao" Optimization control of STATCOM in power system with Adaptive Critic Designs "Third International Workshop on advanced Computational Intelligence (IWACI 2010), pp. 122-126, 2010.

[12] Yu Lei ; Zhang Jianhua and Jiang Cheng"D-STATCOM control based on self-tuning PI with neural networks " China International Conference on Electricity Distribution (CICED), 2012, pp. 1-4, 2012.

[13] Singh, Bhim ; Arya, Sabha Raj ; Dube, Sunil K. ; Chandra, Ambrish and Al-Haddad, Kamal" Implementation of DSTATCOM using Neural Network Based Radial Basis Function "IEEE Industry Applications Society Annual Meeting 2013, pp. 1-8, 2013.

[14] Ghafouri, A. ; Zolghadri, M.R. and Ehsan, M." Power System Stability Improvement Using Self-Tuning Fuzzy Logic Controlled STATCOM "The International Conference on "Computer as a Tool" EUROCON, 2007, pp. 1444-1449, 2007.

[15] Oliver, P.M. ; Ramirez, J.M. ; Pavel, Z.H.and Ruben, T.O." StatCom's Control by neural networks: Results on a lab prototype "IEEE Bucharest Power Tech, 2009 , pp. 1-6, 2009.

[16] Mohagheghi, S. ; Harley, R.G. and Venayagamoothy, G.K. "Intelligent control schemes for a static compensator connected to a power network "Second International Conference on Power Electronics, Machines and Drives, 2004, PEMD 2004, vol. 2, pp. 594-599, 2004.

[17] Wei Qiao ; Harley, R.G. and Venayagamoorthy, G." Coordinated reactive power control of a large wind farm and a STATCOM using heuristic dynamic programming " IEEE Power & Energy Society General Meeting, 2009. PES '09, pp. 1-4, 2009.

[18] Tapia, O.R. ; Zuiga, H.P. and Ramirez, J.M." Neural-based Predictive Control Applied to FACTS Devices " 38th North American Power Symposium, 2006. NAPS 2006, pp. 325-333, 2006.

[19] Voraphonpiput, N. and Chatratana, S." STATCOM Analysis and Controller Design for Power System Voltage Regulation "IEEE/PES Transmission and Distribution Conference and Exhibition : Asia and Pacific, 2005, pp. 1-6, 2005 .

[20] Xinlong L. ; Rui Wang ; Xueguang Zhang and Dianguo Xu "Gain scheduling PD controller for variable pitch wind turbines "7th International Power Electronics and Motion Control Conference (IPEMC), 2012 , vol. 3, pp. 2162-2167, 2012.

[21] Kadri, M.B. ; Khan, S."Fuzzy adaptive pitch controller of a wind turbine "15th International Multitopic Conference (INMIC), 2012, pp. 105-110, 2012.

[22] Poggio, T. and Girosi, F. " Network for approximation and learning " Proceedings of IEEE, vol. 78, pp. 1481-1497, 1989.

[23] Warwick, K. and Irwin, R. G. " Neural network engineering in dynamic control systems" Springer, 1995.